SCIENCEFORECAST
Connecting Research to Drive Scientific Innovation

Research Article
Published: 02 Jul, 2018

SF Journal of Material and Chemical Engineering

Effects of Vacuum and Flow Rate on Water Deoxygenation through Tri-Bore PVDF Hollow Fiber Membranes

Su J*

School of Life Sciences & Chemical Technology, Ngee Ann Polytechnic, 535 Clementi Road, Singapore

Abstract

Novel tri-bore hollow fiber membranes have been prepared for the removal of dissolved oxygen from water. The morphology of the membranes is studied. Two membrane modules are fabricated, each containing 200 pieces of hollow fibers with effective length of 24cm. Deoxygenation experiments are carried out by connecting the two membrane modules in series and continuously flowing normal city water in the fiber lumen side and applying vacuum in the shell side. The concentration of dissolved oxygen before and after the membrane modules is monitored. The effects of vacuum level and water flow rate on the oxygen separation efficiency are examined. Mathematical modeling is conducted to determine the individual mass transfer coefficients at the liquid phase and across the membrane as well as the overall mass transfer coefficient. The concentration profiles of dissolved oxygen along radial and axial directions in the membrane lumen side are also calculated. The influences of water flow rate and vacuum level on the concentration profiles have been investigated. The study not only discloses the potential of the newly developed tri-bore hollow fiber membranes for water degassing applications but also provides valuable analyses on the mass transfer in the deoxygenation process.

Keywords: Tri-bore hollow fiber; Deoxygenation; Vacuum; Flow rate; Concentration profile; Mass transfer

Introduction

Removal of dissolved oxygen from water is an important step for protecting the equipment from corrosion in power industry or enhancing the product quality in pharmaceutical, food and semiconductor industries [1,2]. Conventional methods for deoxygenation include vacuum tower, forced draft degasifies, steam deaerators and chemical reagents. The interest in deoxygenation through hollow fiber membranes has been steadily increasing during the past decade due to their high efficiency as well as energy, space and cost savings [3]. Hollow fiber membranes for deoxygenation are preferentially made of polypropylene (PP), polyvinylidene fluoride (PVDF) and polytetrafluoroethylene (PTFE) [4]. Being hydrophobic, these membranes do not allow liquid water to pass through in case the pressure of the feed water is below the breakthrough pressure, i.e., Liquid Entry Pressure (LEP), which could be correlated with the membrane structure via the Cantor-Laplace equation:

$$LEP = \frac{-2\gamma\cos\theta}{r_{\max}} \qquad (1)$$

where γ is the surface tension of the wetting liquid (in this case water at 25°C, 0.07199 N•m^{-1}), θ is the contact angle between the membrane and the wetting liquid (water), and r_{max} is the maximum radius of the membrane pores.

In hollow fiber membrane modules for deoxygenation, liquid water flows in the lumen or shell side while the other side is under vacuum. To enhance the efficiency, vacuum plus sweeping with high purity nitrogen gas could be used. The transport of oxygen through hydrophobic membrane is illustrated in Figure 1.

The overall resistance to the transport of oxygen could be expressed using the resistance-in-series concept [5]:

$$\frac{1}{K} = \frac{1}{k_L} + \frac{RTd_i}{Hk_M d_m} + \frac{d_i}{Hk_G d_O} \qquad (2)$$

where K, k_L, k_M and k_G are the overall mass transfer coefficient and individual mass transfer coefficients at the liquid phase, membrane and gas phase, respectively; d_i, d_m and d_o are inner, logarithmic mean and outer diameters of the hollow fiber, respectively. At the side under vacuum, the resistance is negligible and the element $d_i/(Hk_G d_o)$ can be ignored [6]. When water flows in the lumen side of

OPEN ACCESS

Correspondence:
J. Su, School of Life Sciences & Chemical Technology, Ngee Ann Polytechnic, 535 Clementi Road, Singapore.
E-mail: *SU_Jincai@np.edu.sg*

Received Date: *08 May 2018*
Accepted Date: *26 Jun 2018*
Published Date: *02 Jul 2018*

Citation: *Su J. Effects of Vacuum and Flow Rate on Water Deoxygenation through Tri-Bore PVDF Hollow Fiber Membranes. SF J Mater Chem Eng. 2018; 1(2): 1010.*

ISSN 2643-8100

Copyright *© 2018 Su J. This is an open access article distributed under the Creative Commons Attribution License, which permits unrestricted use, distribution, and reproduction in any medium, provided the original work is properly cited.*

hollow fibers, the flow rate of water influences the mass transfer coefficient and k_L might dominate K [7]. Pilot-scale testing conducted by Peng et al. supports the above statement [1]. In the study by Tan et al., water vapor permeation in vacuum deoxygenation was found to enhance the mass transfer of oxygen across the membrane, thus favoring the removal of oxygen.

In a recent work, robust tri-bore PVDF hollow fiber membranes were used for the control of dissolved oxygen in aquaculture denitrification system [8]. With water flowing in the lumen side and vacuum in the shell side, the membrane performance was found to vary with water flow rate and vacuum level. To investigate their influence on the mass transport of oxygen, deoxygenation experiments were designed and carried out in this study. The efficiency for the oxygen removal was determined. Mathematic modeling was conducted to examine the radial and axial change in the concentration of oxygen. Considering the continuous testing and the large quantity of water used, normal city water instead of aquaculture water was used.

Experimental

Membrane materials

Two 1.5 inch membrane modules were connected in series and used for deoxygenation experiments. Each module (Figure 2) contains 200 pieces of freeze-dried PVDF tri-bore hollow fibers with the two ends sealed using epoxy resin. The tri-bore hollow fibers were produced via a dry-jet wet phase inversion spinning process and detailed spinning conditions were documented elsewhere [Su and Wei, 2018]. The effect length of the hollow fibers in each membrane module is 24cm. The morphology of the PVDF hollow fiber membranes was inspected using a Field Emission Scanning Electron Microscope (FESEM, JEOL JSM-7600F, Japan). For FESEM inspection, the membrane samples were fractured and coated with platinum using a sputtering coater (JEOL JFC-1600, Japan).

Deoxygenation experiments

The two membrane modules was mounted into a lab-scale experimental setup (Figure 3) and examined for deoxygenation. City water was continuously introduced to the lumen side of the hollow fiber membranes at room temperature (25°C) and was drained after passing through the Aqua sensor (Thermo Scientific). The flow rate, pressure and concentration of dissolved oxygen before and after the membrane modules were monitored throughout the experiment. Vacuum was applied at the membrane shell side while the vacuum level was controlled at different levels.

Two sets of experiment were carried out. For the first set of experiment, city water was controlled at different flow rates, i.e., 20, 100, 300, 500, 700 and 900 mL•min^{-1}, respectively, with the shell side at the same vacuum of 29 inHg. For the second set of experiment, the vacuum level at the shell side was controlled at 11, 14, 17, 20, 23, 26 and 29 inHg. The efficiency (E) of deoxygenation is expressed as

$$E = \left(1 - \frac{C_{out}^{l}}{C_{in}^{l}}\right) \times 100\% \qquad (3)$$

where C_{in}^{l} and C_{out}^{l} are the concentrations of dissolved oxygen in water at the inlet and outlet of the membrane, respectively.

Mass transfer coefficient

The mass transfer coefficient in the liquid phase can be calculated from Leveque equation:

$$\frac{k_i d_i}{D_i} = 1.62\left(\frac{d_i \bar{v}}{L D_l}\right)^{\frac{1}{3}} \qquad (4)$$

The mass transfer coefficient in the hydrophobic membrane is [5]:

$$k_M = D_p \left\{\frac{\varepsilon}{\tau b}\right\} \qquad (5)$$

where D_p, τ, and b denote the diffusivity of oxygen in the membrane pore, the tortuosity of the pore and the membrane thickness, respectively. In the membrane pores, the transport of oxygen is through Knudsen diffusion and the diffusivity can be estimated using the following equation:

$$D_p = \frac{d_p}{3}\left(\frac{8RT}{\pi M_w}\right)^{\frac{1}{2}} \qquad (6)$$

where D_p is the mean pore diameter and M_w is the molecular weight of oxygen.

Concentration profile of oxygen

Figure 1 is a schematic diagram of the transport of oxygen with water flowing in the lumen side of the hollow fiber membrane as well as the concentration profile at different phases. The steady state two-dimensional flow in the lumen side can be written as [9-11].

$$v_z \frac{\partial C}{\partial z} = D_l \frac{\partial^2 C}{\partial z^2} + \frac{D}{r}\frac{\partial}{\partial r}\left(r\frac{\partial C}{\partial r}\right) \qquad (7)$$

where C, D_l, r and v_z denote the local concentration of oxygen, the diffusivity of oxygen in water, the radial distance and the axial velocity of water. The velocity profile in z direction can be obtained as:

$$v_z(r) = 2\bar{v}\left\{1 - \left(\frac{r}{R}\right)^2\right\} \qquad (8)$$

where $\bar{v}$ is the average velocity of water in the lumen and R is the radius of the fiber lumen. The boundary conditions for equation (6) are as follows:

$$z=0,\ C_{(r,0)} = C_{in,b}$$
$$r=0,\ C_{(0,z)} = 0 \text{ is finite or } \left[\frac{\partial C}{\partial r}\right]_{o,z} = 0 \qquad (9)$$
$$C_{(R,z)} = C_R = C_i$$

The following dimensionless form could be considered to express equation (7)

$$\theta = \frac{C - C_i}{C_o - C_i},\ Y = \frac{r}{R},\ Z = \frac{z}{RP_e} \qquad (10)$$

where P_e is the Peclet number defined as $P_e = Rv_0/D$. Substituting these dimensionless variables into equation (7) gives

$$\left(1 - Y^2\right)\frac{\partial \theta}{\partial Z} = \frac{1}{Pe^2}\frac{\partial^2 \theta}{\partial Z^2} + \frac{1}{Y}\frac{\partial}{\partial Y}\left(Y\frac{\partial \theta}{\partial Y}\right) \qquad (11)$$

Boundary conditions for equation (11) are as follows:

$$\theta(Y,0)=1,\ \theta(1,Z)=0,\ \theta(0,Z) \text{ is finite or } \frac{\partial \theta}{\partial Y}(0,Z) = 0 \qquad (12)$$

The values for P_e are generally large (P_e >100). Therefore, it is valid to assume $\frac{1}{Pe^2} \ll 1$ and $\frac{1}{Pe^2}\frac{\partial^2 \theta}{\partial Z^2} \approx 0$. Neglecting the item $\frac{1}{Pe^2}\frac{\partial^2 \theta}{\partial Z^2}$ in equation (11), the solution of the simplified equation is:

$$\theta(Y,Z) = \sum_{n=1}^{\infty} A_n e^{-\lambda_n^2 Z} \Phi_n(Y) \qquad (13)$$

In equation (13), $\Phi_n(Y)$ is the eigen function of a proper Sturm-Liouville system:

$$\lambda^2\left(1 - Y^2\right)\Phi + \frac{1}{Y}\frac{\partial}{\partial Y}\left(Y\frac{\partial \Phi}{\partial Y}\right) = 0 \qquad (14)$$

Boundary conditions of equation (14) are

$$\frac{d\Phi}{dY}(0) = 0 \text{ or } \Phi(0) \text{ is finite;}\ \Phi(1)=0 \qquad (15)$$

Defining $X=\lambda Y^2$ and substituting it into equation (14) gives

$$X\frac{\partial^2 W}{\partial X^2} + (1 - X)\frac{dW}{dX} + \left(\frac{\lambda}{4} - \frac{1}{2}\right)W = 0 \qquad (16)$$

Equation (16) is Known as Kummer's equation and has two

solutions, i.e., the Kummer function of the first kind $M\left(\frac{1}{2}-\frac{\lambda}{4},1,X\right)$ and the Tricomi function $T\left(\frac{1}{2}-\frac{\lambda}{4},1,X\right)$ considering the boundary condition of $\Phi(0)$and $W(0)$, only $M\left(\frac{1}{2}-\frac{\lambda}{4},1,X\right)$ is the valid solution of equation (16):

$$W(X)=M\left(\frac{1}{2}-\frac{\lambda}{4},1,X\right)$$

$$M\left(\frac{1}{2}-\frac{\lambda}{4},1,X\right)=1+\frac{a}{b}X+\frac{a(a+1)X^2}{b(b+1)2!}+\cdots+\frac{a(a+1)\cdots(a+n-1)X^n}{b(b+1)\cdots(b+n-1)n!}+\cdots \quad (17)$$

(18)

where $a=\frac{1}{2}-\frac{\lambda}{4}$ and $b=1$. The item A_n in equation (13) might be determined by:

$$A_n=\frac{\int_0^1\Phi_n(Y)Y(1-Y^2)dY}{\int_0^1\Phi_n^2(Y)Y(1-Y^2)dY} \quad (19)$$

The value of λ could be determined as follows:

$$\Phi(Y)=e^{-\frac{\lambda Y^2}{2}}W(\lambda Y^2) \text{ at } \Phi(1)=0 \quad (20)$$

Results and Discussion

Membrane morphology

The tri-bore hollow fibers have a triangular shape with the fiber wall and the junction at the center having thickness of about 120 and 200 μm, respectively (Figure 2). The thin fiber wall is favorable for the reduction in the resistance to oxygen transport while the relative thicker junction provides strong support to the membrane in order to maintain its integrity. Each fiber has three flow channels, each of which has an average diameter of about 670 μm. To efficiently utilize the membrane area, the feed water for deoxygenation experiments was run inside the hollow fibers. The inner surface of the hollow fiber membranes is apparently porous which is favorable for the transport of oxygen. The outer surfaces are less porous, consisting of interconnected globules. The pores within the inner skin layer of the tri-bore hollow fiber membranes are in the range of 2-20 nm and the mean pore radius is 6.3nm [8]. The membranes are in the category of ultrafiltration and the LEP value for water is determined at 9.9 bar.

Performance of water deoxygenation

In the fiber lumen side, dissolved oxygen needs to diffuse in liquid water towards the water-gas interface and pass through the interface before entering the membrane pores as gas molecules. Oxygen molecules are immediately taken away upon continuous suction in the shell side. In the deoxygenation experiment, the water flow rate was found to influence the oxygen removal efficiency E (Figure 4). Interestingly, the increase in the water flow rate results in higher deoxygenation efficiency and reaches a maximum value of 85.95% at

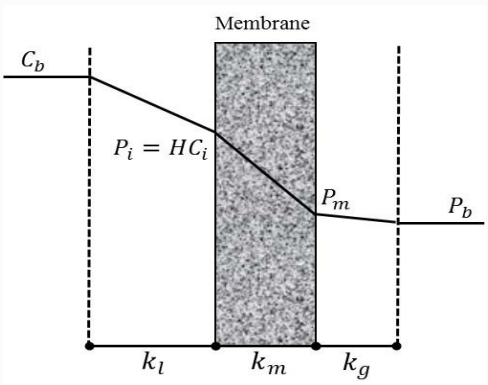

Figure 1: Transport of oxygen through a hydrophobic membrane.

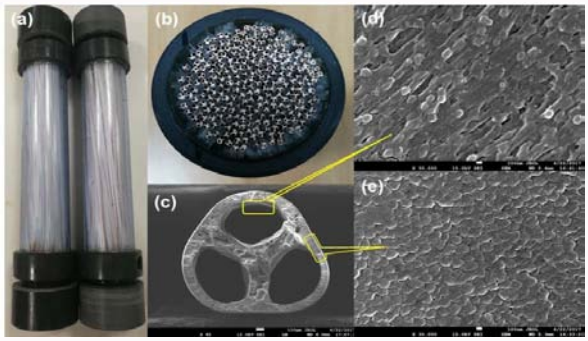

Figure 2: Membrane modules (a), top view of the module (b), cross section of the tri-bore hollow fiber (c) and its inner surface (d) and outer surface (e).

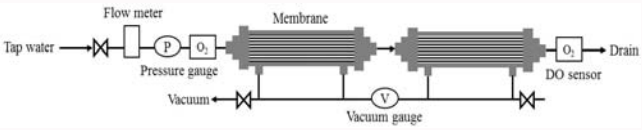

Figure 3: Schematic diagram of the deoxygenation system.

300 mL•min^{-1}. Thereafter, the efficiency drops with further increase in the water flow rate. At the highest water flow rate (900 mL•min^{-1}) tested in the experiment, the oxygen removal efficiency decreases to 66.75%.

For all the experiments, the feed water is absolutely under laminar flow with Reynolds number in the range of 0.54-29.72 (Table 1). k_M is always higher than k_L at all water flow rates. With increasing the water flow rate, k_L increases significantly while k_M does not change much. Within the membrane matrix, the resistance to the movement of oxygen molecules comes from the tortuous or interconnected pore walls. Being hydrophobic, the hollow fiber membrane does not allow liquid water to enter the pores. Therefore, varying the water flow rate does not apparently influence the transport of oxygen across the membrane pores. The slight change in k_M might be caused by the change in the temperature due to coupling effect of water evaporation at the water-gas interface as well as the condensation of water vapor in the membrane shell side.

The resistance to oxygen transport at different flow rates is shown in Figure 5. With increasing the water flow rate, the resistance at the liquid phase ($1/k_L$) decreases significantly. Though at laminar flow, faster water flow makes the bounder layer near the inner surface thinner and favors the transport of oxygen to the gas-liquid interface at the aperture of the membrane pores. However, the increase in the water flow rate hardly influences the resistance of the membrane matrix as liquid water cannot enter the membrane pores. In other words, the flow path for oxygen (i.e., membrane pores) remains intact. It is also noticed that the resistance at the liquid phase ($1/k_L$) is much higher than that in the membrane (RTd_i/Hk_Md_m). Therefore, the transport of oxygen in the liquid phase dominates the rate of deoxygenation.

The deoxygenation experiments began at 29 inHg vacuum in the shell side. The exiting concentration of dissolved oxygen gradually reduced and would stabilize at a certain level. After maintaining at the same oxygen concentration for at least 30min, the experiment proceeded to the next vacuum level. Using 300 mL•min^{-1} as an example, the influence of vacuum on the efficiency of oxygen removal is shown in Figure 6. Obviously, better efficiency is achieved at

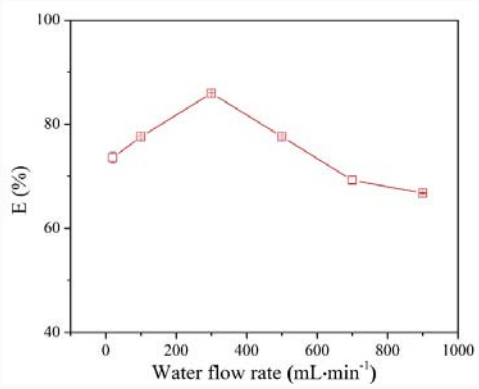

Figure 4: Effect of the water flow rate on the oxygen removal efficiency.

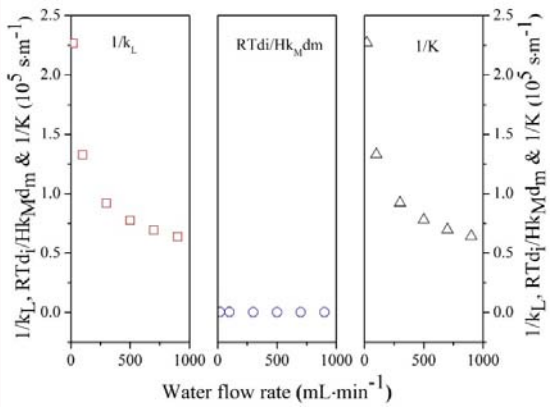

Figure 5: Resistance to oxygen transport at different water flow rates.

increased vacuum levels. Vacuum level in the shell side is not supposed to influence the diffusion of oxygen within the liquid water. At higher vacuum level, the partial pressure of oxygen in the shell side, within the membrane as well as at the water-gas interface is lower. This might have created larger driving force for the transport of oxygen from liquid water to the gas phase (under vacuum). Additionally, higher vacuum level accelerates the rate of water evaporation at the water-gas interface, which in turn enhances the transport of oxygen [2].

Condensation of water vapor happens at the inner wall of the transparent membrane housing, and the condensed water would not disappear even when the deoxygenation experiment is completed (Figure 7(a)). Evaporation of water consumes energy and it tends to cool down the liquid water flowing inside the hollow fibers. Condensation of water vapor happens at the shell side, releasing thermal energy and tending to heat up the hollow fiber and the liquid water in the lumen side. Surprisingly, the change in the vacuum shows different influences on the exiting temperature of the liquid water at different water flow rates (Figure 7(b)). When water flows slowly (e.g. 20 mL•min^{-1}), it is gradually cooled down when evaporation absorbs thermal energy. As PVDF is a poor conductor, the heat transfer rate through the fiber wall is slow. Thus, the influence of the thermal energy released from water vapor condensation at the other side of the membrane is much weaker than the cooling effect and this might explain the slight decrease in the exiting temperature of the liquid water at all vacuum levels. At medium flow rate (e.g. 300 mL•min^{-1}), more condensed water could be seen on the inner wall of the membrane housing. The exiting temperature of water slightly increases with reducing the vacuum level and then drops after

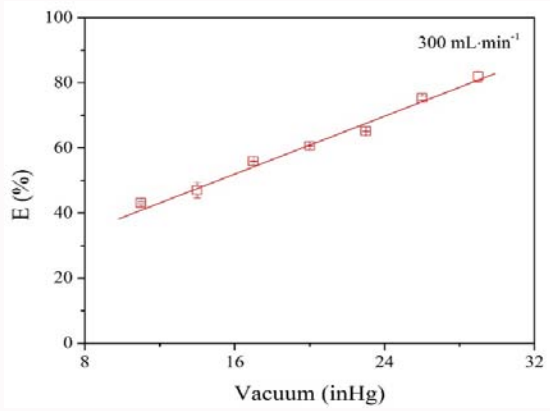

Figure 6: Effect of vacuum on the deoxygenation efficiency.

reaching a maximum value at 20 inHg vacuum. The difference in the exiting temperature of water at 900 mL•min^{-1} is more obvious. At this water flow rate, more water vapor is generated but the liquid water stays within the membrane module much shorter and the cooling effect lags behind. Condensation of the large quantity of water vapor at high vacuum level releases a lot of thermal energy which heats up the whole membrane module. This is why the exiting temperature of water slightly increases though decreasing the vacuum level from 29 to 26 and 23 inHg at 900 mL•min^{-1}. Further decreasing the vacuum level, less water vapor forms and condenses in the membrane shell side and less thermal energy is released. Heating effect is still competing with the cooling effect but its influence becomes minor. As a result, the exiting temperature of the liquid water decreases. As it is not possible to avoid the evaporation of the liquid water and the condensation of water vapor, their influence on the deoxygenation has to be considered. Further study is to be carried out to investigate the water evaporation rate at various operation conditions and the long term influence of water vapor condensation on the mass transfer rate.

Concentration profiles

The concentration of dissolved oxygen at radial and axial directions within the membrane module has been calculated using equations (7)-(20). The trend of concentration profiles is similar. As an example, the radial and concentration profiles at 300 and 900 mL•min^{-1}flow rates and three different vacuum levels are presented and discussed here (Figure 8). As seen from Figure 8(a), the concentration of dissolved oxygen is the highest at the center of the hollow fiber for both flow rates while it decreases along the radial direction towards the fiber wall. The concentration gradient in the radial direction is small at low vacuum level and it becomes larger with increasing the vacuum level. At the same vacuum level, the concentration of dissolved oxygen drops faster near the fiber center area at 300 mL•min^{-1} than 900 mL•min^{-1}. However, the concentration

Table 1: Reynolds number and mass transfer coefficients at different water flow rates.

Parameter	Water flow rate (mL·min^{-1})					
	20	100	300	500	700	900
Re	0.54	2.71	8.62	14.37	20.12	29.72
k_L (×10^6 m·s^{-1})	4.41	7.54	10.87	12.90	14.42	15.69
k_M (×10^5 m·s^{-1})	6.43	6.44	6.45	6.46	6.47	6.53
K (×10^6 m·s^{-1})	4.40	7.52	10.84	12.84	14.36	15.61

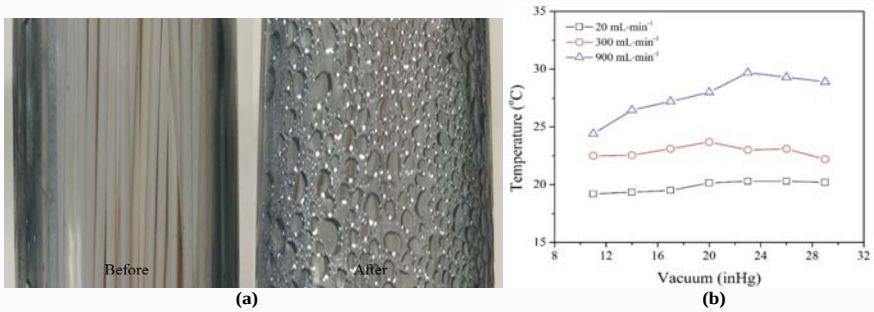

(a) (b)

Figure 7: Membrane module before and after the deoxygenation experiment (a) and exiting temperature of water (b).

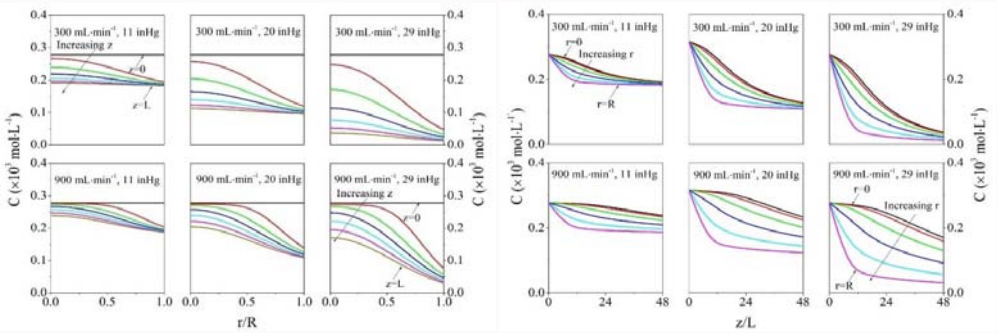

(a) (b)

Figure 8: Radial concentration profiles (a) and axial concentration profiles (b) at different vacuum levels (11, 20 and 29 inHg) and water flow rates (300 and 900 mL·min^{-1}).

of dissolved oxygen drops more rapidly near the fiber wall area at 900 mL•min^{-1}. Thinner boundary layer and reduced resistance to oxygen transport at increased water flow rate account for the phenomenon. Furthermore, the transport of dissolved oxygen from the liquid bulk to the fiber wall area limits the overall mass transfer rate. A relatively slow water flow rate of 300 mL•min^{-1} results in better deoxygenation performance.

As shown in Figure 8(b), the influence of the water flow rate and vacuum level on the axial concentration profiles is also quite significant. The concentration profile of dissolved oxygen is only slightly different near the entering of the membrane module at both flow rates but the difference becomes more obvious along the membrane module. The axial concentration profiles at different r/R locations becomes dispersed with increasing the vacuum level while the distribution becomes more broad at 900 mL•min^{-1} water flow rate. After the first membrane module (24 cm), the concentrations of dissolved oxygen are close to exiting values at different r/R locations for 300 mL•min^{-1} flow rate. However, they are still pretty dispersed at 900 mL•min^{-1} at any vacuum level. The effect of the vacuum level on the oxygen removal efficiency seems to be more significant at enhanced water flow rates. From this aspect, the membrane module could be longer if operating at relatively high water flow rates.

Conclusions

Tri-bore hollow fiber membrane modules have been fabricated for water deoxygenation. The morphology of the membranes is studied. The influences of the water flow rate and vacuum level on the oxygen removal efficiency have been studied. It is found that too slow (e.g. 20 mL•min^{-1}) or too high flow rate (e.g. 900 mL•min^{-1}) does not favor the deoxygenation performance and a medium flow rate (e.g. 300 mL•min^{-1}) is preferable. The highest oxygen removal efficiency is 82% achieved at 300 mL•min^{-1} and 29 inHg vacuum. Water evaporation and water vapor condensation affect the deoxygenation performance but both are not avoidable for vacuum degassing systems. The liquid water temperature would be dropping if the membrane module is operated at low flow rate due to their opposite influences.

Mathematical modeling is also carried out to investigate the transport of oxygen from water to the gas phase through the membrane. The resistance to oxygen transport mainly lies in the liquid phase while the resistance created by the liquid water is 200-668 times of that created by the membrane. Either the vacuum level or the water flow rate influences radial and axial concentration profiles of dissolved oxygen within the liquid phase. The best performance appears at medium water flow rate and enhanced vacuum level.

Acknowledgement

We acknowledge Singapore Ministry of Education and Ngee Ann Polytechnic for funding the research through the projects "High throughput multi-bore hollow fiber membrane module for deoyxgenation" (Grant number MOE2014-TIF-1-G-020) and "A low cost membrane-assisted denitrification system for zero-discharge recirculating aquaculture" (16GAP003). Thanks are also due to Center of Innovation Environmental and Water Technology, Ngee Ann Polytechnic for the equipment for membrane morphology inspection.

References

1. Peng ZG, Lee SH, Zhou T, Shieh JJ, Chung TS. A study on pilot-scale degassing by polypropylene (PP) hollow fiber membrane modules. Desalination. 2008; 234: 316–322.

2. Tan X, Capar G,Li K. Analysis of dissolved oxygen removal in hollow fiber membrane modules: effect of water vapour. J. Membr. Sci. 2005; 251:

111–119.

3. Martic I, Maslarevic A, Mladenovic S, Lukic U, Budimir S. Water deoxygenation using hollow fiber membrane module with nitrogen as inert gas. Desalination and Water Treatment. 2014; 54: 1–5.

4. Bhaumik D, Majumdar S, Fan Q, Sirkar KK. Hollow fiber membrane degassing in ultrapure water and microbiocontamination. J. Membr. Sci. 2004; 235: 31–41.

5. Drioli E, Curcio E, Di Profio G. State of the art and recent progresses in membrane modules. Chem. Eng. Res. Des. 2005; 83: 223–233.

6. Li J, Zhu LP, Xu YY, Zhu BK. Oxygen transfer characteristics of hydrophilic treated polypropylene hollow fiber membranes for bubbles aeration. J. Membr. Sci. 2010; 362: 47–57.

7. Yang MC, Cussler EL. Designing hollow-fiber modules. AlChE J. 1986; 32: 1910–1916.

8. Su J, Wei Y. Novel tri-bore PVDF hollow fiber membranes for the control of dissolved oxygen in aquaculture water. J. Water Process Eng. 2018.

9. Mandowara A, Bhattacharya PK. Membrane module as degasser operated under vacuum for ammonia removal from water: A numerical simulation of mass transfer under laminar flow conditions. Comput. Chem. Eng. 2009; 33: 1123–1131.

10. Kieffer R, Charcosset C, Puel F, Mangin D. Numerical simulation of mass transfer in a liquid-liquid membrane module for laminar flow conditions. Comput. Chem. Eng. 2008; 32: 1325–1333.

11. Treybal RE. Mass-transfer operations. Singapore: McGraw-Hill International Editions. 1981.